Disruption of *MAPK1* expression in the ERK signalling pathway and the RUNX1-RUNX1T1 fusion gene attenuate the differentiation and proliferation and induces the growth arrest in t(8;21) leukaemia cells

SALEM ALI AL-SALEM BASHANFER[2], MOHAMED SALEEM[3], OLAF HEIDENREICH[4], EMMANUEL JAIRAJ MOSES[1] and NARAZAH MOHD YUSOFF[1]

[1]Advanced Medical and Dental Institute, Universiti Sains Malaysia, Bertam, Kepala Batas, Pulau Pinang 13200, Malaysia; [2]Hematology Department, College of Medicine and Health Sciences, University of Hodiedah, Hodiedah 3730, Yemen; [3]Advanced Genomics Lab Sdn Bhd, Kota Damansara, Petaling Jaya, Selangor Darul Ehsan 47810, Malaysia; [4]Northern Institute for Cancer Research, Medical School, Newcastle upon Tyne NE2 4HH, UK

Received June 28, 2017; Accepted June 8, 2018

DOI: 10.3892/or.2018.6926

Abstract. The t(8;21) translocation is one of the most frequent chromosome abnormalities associated with acute myeloid leukaemia (AML). This abberation deregulates numerous molecular pathways including the ERK signalling pathway among others. Therefore, the aim of the present study was to investigate the gene expression patterns following siRNA-mediated suppression of *RUNX1-RUNX1T1* and *MAPK1* in Kasumi-1 and SKNO-1 cells and to determine the differentially expressed genes in enriched biological pathways. BeadChip microarray and gene ontology analysis revealed that *RUNX1-RUNX1T1* and *MAPK1* suppression reduced the proliferation rate of the t(8;21) cells with deregulated expression of several classical positive regulator genes that are otherwise known to enhance cell proliferation. *RUNX1-RUNX1T1* suppression exerted an anti-apoptotic effect through the overexpression of *BCL2*, *BIRC3* and *CFLAR* genes, while MAPK1 suppression induced apopotosis in t(8;21) cells by the apoptotic mitochondrial changes stimulated by the activity of upregulated *TP53* and *TNFSF10,* and downregulated *JUN* gene. *RUNX1-RUNX1T1* suppression supported myeloid differentiation by the differential expression of *CEBPA*, *CEBPE*, *ID2*, *JMJD6*, *IKZF1*, *CBFB*, *KIT* and *CDK6*, while *MAPK1* depletion inhibited the differentiation of t(8;21) cells by elevated expression of *ADA* and downregulation of *JUN*. *RUNX1-RUNX1T1* and *MAPK1* depletion induced cell cycle arrest at the G_0/G_1 phase. Accumulation of cells in the G_1 phase was largely the result of downregulated expression of *TBRG4*, *CCNE2*, *FOXO4*, *CDK6*, *ING4*, *IL8*, *MAD2L1* and *CCNG2* in the case of *RUNX1-RUNX1T1* depletion and increased expression of *RASSF1*, *FBXO6*, *DADD45A* and *P53* in the case of *MAPK1* depletion. Taken together, the current results demonstrate that MAPK1 promotes myeloid cell proliferation and differentiation simultaneously by cell cycle progression while suppresing apoptosis.

Correspondence to: Professor Narazah Mohd Yusoff or Dr Emmanuel Jairaj Moses, Advanced Medical and Dental Institute, Universiti Sains Malaysia, Bertam, Kepala Batas, Pulau Pinang 13200, Malaysia
E-mail: narazah@usm.my
E-mail: emmanuel_jm@usm.my

Key words: acute myeloid leukaemia, t(8:21), MAPK1, ERK pathway

Introduction

Acute myeloid leukaemia (AML) with karyotypic discernible translocation (t)(8;21)(q22;q22) (*RUNX1-RUNX1T1*) is observed in approximately 7% of adults (1), and is the most frequent non-lymphoblastic leukaemia in children (2). This balanced translocation disrupts two functionally distinct genes, *RUNX1* (previously termed *AML1*) and *RUNX1T1* (commonly known as *ETO* or *MTG8*) (3). Physiologically, *RUNX1* is a transcription factor that encodes to the alpha subunit of the core biding factor (CBFα) which forms a heterodimer with the CBFβ subunit and regulates differentiation of haematopoietic stem cells into committed mature cells. The translocated *RUNX1T1* moiety gets activated as a result of the fusion with *RUNX1* (4,5). Together, the hybridised RUNX1-RUNX1T1 (RR) oncoprotein functions as a dominant negative form of RUNX1. As empirically shown, RR exerts a repressive effect on the promoters of genes normally activated by the RUNX1 transcription factor through interactions of its RUX1T1 moiety with nuclear corepressors such as *NCOR1* and Sin3A (6,7). Several studies have indicated that this altered transcription pattern impairs myeloid precursor cell differentiation, proliferation and apoptosis, and is therefore thought to be the underlying pathogenesis of myeloid leukaemia (8-13). However, this translocation itself is not necessarily sufficient for the development of AML. It appears that additional

secondary mutations are required to impair haematopoietic differentiation to recapitulate the phenotypic features of AML. Based on recent studies there appears to be a fairly consistent association between the t(8;21) translocation and the classical MAPK signalling pathway (9,14).

One of many signalling pathways triggered by haematopoietic cytokines is the ERK (Ras/Raf/MEK/ERK) pathway. The MAP kinase ERK2 (MAPK1), encoded by *MAPK1*, plays an integral role in the ERK cascade in relaying extracellular biological signals from cell membrane to the nucleus. This mechanism modulates the normal haematopoietic cell proliferation, differentiation and prevention of apoptosis (15). The ERK pathway, most extensively studied of all MAPK pathways, is deregulated in a third of all human cancers, a frequent observation in the pathogenesis of haematological malignancies such as AML (16-18). In wide varieties of AMLs, constitutive activation that centres on the MEK/ERK node in the pathway has been attributed to the tumourigenic effects such as independence of proliferation and evasion of apoptosis (16-19). Previous study revealed that AML with t(8;21) encoded RR induces a microRNA-dependent mechanism that utilises the MAPK cascade to signal hyper-proliferation of myeloid progenitors and block their differentiation (20). Another group reported that Kasumi-1 cells that were refractory to apoptosis following *RR* silencing activate an array of signalling pathways involved in cell survival and proliferation, prominently the ERK2 pathway (21). These findings underscore the influence of RR on the MAPK pathway towards the pathobiology of AML.

Although the role of constitutive activation of the MEK/ERK pathway in the development of myeloid leukaemia is well established, RR- and MAPK-driven intricate molecular and cellular pathways that maintain the pathobiology of AML remain elusive. In the present study we used siRNA-mediated gene silencing approach to elucidate the transcription profiles of *RR* and *MAPK1* suppressed AML cell lines and further analysed these expression signatures to explore the molecular mechanisms involved in cell proliferation, cell cycle distribution, apoptosis and differentiation. In the present study, we report differential regulation of gene expression by RR and MAPK1 as determined by genome-wide expression analysis responsible for the phenotypic features of AML.

Materials and methods

Cell culture and siRNA transfection. Two suspension leukaemic cell lines with t(8;21), Kasumi-1 and SKNO-1, were used in the present study. The former was obtained from the American Type Culture Collection (ATCC; Manassas, VA, USA) while the latter was a kind gift from Professor Olaf Heidenreich (Northern Institute for Cancer Research, Newcastle University, UK). Kasumi-1 and SKNO-1 cells were cultured in RPMI-1640 medium containing 10 and 20% foetal bovine serum (FBS) (Gibco; Thermo Fisher Scientific, Inc., Waltham, MA, USA), respectively. SKNO-1 was also supplemented with 10 ng/ml of granulocyte-macrophage colony stimulating factor (GM-CSF). Cell lines were incubated at 37˚C in a humidified incubator with 5% CO_2.

Kasum-1 and SKNO-1 cells cultivated to late log growth phase, concentrated to 10^7 cells/ml in culture medium without serum, were electroporated with siRNA using a Bio-Rad Gene Pulser Xcell™ at 330 V for 10 m. The sequences of siRNAs used are as follows: *si*RNA-*MAPK1* (*siMAPK1*) sense, 5'-GUUCGAGUAGCUAUCAAGATT-3' and antisense, 5'-UCUUGAUAGCUACUCGAACTT-3'; *si*RNA-*RUNX1-RUNX1T1* (*siRR*) sense, 5'-CCUCGAAAU CGUACUGAGAAG-3' and antisense, 5'-UCUCAGUACGAU UUCGAGGUU-3'; and scrambled mismatch *si*RNA (*si*MM) from Qiagen (Hilden, Germany).

For isolated downregulation of *RR* and *MAPK1* gene expression, both cell types were electro-transfected with 200 nM of *siRR* and 100 nM of annealed *siMAPK1* respectively; and for co-transfection a mixture of both *siRR* and *siMAPK1* were used. These concentrations were derived from dose-dependent experiments performed in our laboratory. In experiments requiring extended transfection, cells were sequentially transfected on days 0, 4 and 7. Immediately after electro-transfection, cells were diluted 20-fold in complete culture medium and returned to the incubator. All cell groups were electroporated in triplicates.

RNA isolation and integrity evaluation. Quantitative RT-PCR total RNA was isolated using RNeasy Mini kit (Qiagen) according to the manufacturer's protocol. RNA integrity was analysed on an Agilent 2100 Bioanalyser RNA 6000 NanoLabChip (Agilent Technologies, Palo Alto, CA, USA) to produce an electrophoresis trace of 18S and 28S peaks using 2100 Expert Software (Agilent Technologies). The RNA integrity number (RIN) was calculated directly from the peak areas, a value of 10 corresponded to intact RNA while 1 indicates a total degradation. Our optimised methods showed a 28S:18S ratio of 1.9-2.1:1 and an RIN of 9-10.

Quantitative real-time polymerase chain reaction (q-RT-PCR). Quantitative real-time-polymerase chain reaction (qRT-PCR) was performed on RNA isolated at various time points post-transfection to quantify the mRNA expression levels of *MAPK1* and *RR* genes in cells treated with respective siRNAs.

Gene-specific primers for *MAPK1* (forward, 5'-CTGCTG CTCAACACCACCT-3' and reverse, 5'-GCCACATATTCT GTCAGGAACC-3'); and *B2M* (forward, 5'-GGCATTCCT GAAGCTGACAG-3' and reverse, 5'-TCTGCTGGATGA CGTGAGTAA-3') were designed using PrimerPlex software (Premier Biosoft, Palo Alto, CA, USA). Primers to quantify *RR* expression were: Forward, 5'-AATCACAGTGGATGG GCCC-3' and reverse, 5'-TGCGTCTTCACATCCACAGG-3' as described by Heidenreich *et al* (5).

A mixture of 50 ng of total RNA together with 0.5 μM of *MAPK1* and *B2M*, and 0.2 μM of *RR* primers was reverse transcribed and amplified simultaneously in the same reaction tube using the QuantiFast SYBR®-Green RT-PCR One-Step PCR Master Mix (Qiagen) in a final volume of 20 μl on a StepOnePlus Real-Rime thermocycler (Applied Biosystems; Thermo Fisher Scientific, Inc., Waltham, MA, USA). The thermocycler was programmed at 50˚C for 10 min for RNA reverse transcription into complementary cDNA followed by 95˚C for 5 min for the initial DNA polymerase activation step. Quantitative amplification was carried out in 35 cycles of denaturation at 95˚C for 10 sec, and annealing and extension at 60˚C for 30 sec. All reactions were performed in triplicates.

Relative quantity of *MAPK1* and *RR* mRNA expression was computed using the comparative cycle threshold ($2^{-\Delta\Delta Ct}$) method normalised with the β_2 microglobulin *B2M* expression as endogenous reference gene. Mock cells were used as a reference sample for normalisation and AllStars negative siRNA (Qiagen) as a mismatch (siMM) control for validation purposes.

Cellular differentiation assay. Differentiation ability of *RR*- and *MAPK1*-suppressed Kasumi-1 cells was monitored by CD34 expression. Kasumi-1 cells sequentially transfected on days 0, 4 and 7 with either *siRR*, *siMAPK1* or a combination of *siRR*+*siMAPK1* were double stained on day 9 with allophycocyanin conjugated anti-CD34:APC and peridinin-chlorophyll A protein conjugated anti-CD45:PerCP (Becton-Dickinson, Franklin Lakes, NJ, USA).

Briefly, ~10^5 transfected Kasumi-1 cells were treated with Fc blocking reagent [phosphate-buffered saline (PBS) containing 0.02% sodium azide and 1% BSA] and incubated on ice for 30 min to block non-specific antibody binding. After incubation, the cells were washed and re-suspended in 100 μl of PBS. Cells were subsequently stained with 0.5 μl of allophycocyanin conjugated anti-CD34:APC and 2 μl of peridinin-chlorophyll A protein conjugated anti-CD45:PerCP (Becton-Dickinson). Cells were sorted on a FACSCanto II equipped with BD FACSCanto Clinical Software for acquisition and analyses. Mock cells and siMM-transfected Kasumi-1 cells were used as controls.

Cell apoptosis assay. To determine the suppressive effects of *MAPK1* and *RUNX1-RUNX1T1* genes on apoptosis induction, Kasumi-1 cells were sequentially transfected on days 0, 4 and 7 with *siMAPK1* and *siRR* singly, and in combination. Apoptosis was quantified on day 9 using an Annexin V/fluorescein isothiocyanate (FITC) assay kit (AbD Serotec®; Bio-Rad Laboratories, Raleigh, NC, USA) using a FACSCanto™ II (BD Biosciences; Becton-Dickinson and Company, Franklin Lakes, NJ, USA) flow cytometer. In brief, cells in logarithmic growth phase after treatment with siRNA were washed once in cold 1X PBS and once in cold 1X binding buffer. Cells were suspended to a density of 1x10^5 cells in 100 μl of 1X binding buffer and treated with 5 μl of Annexin V:FITC for 10 min in the dark at room temperature. On completion, the cells were washed again in 1X binding buffer and re-suspended in 190 μl of 1X binding buffer with 10 μl of propidium iodide (PI) and directly analysed on a flow cytometer. siMM-transfected cells were used as a negative control.

Cell cycle analysis. Distribution of Kasumi-1 cells in different phases of the cell cycle were examined using EZCell™ cell cycle analysis kit (BioVision, Milpitas, CA, USA) according to the manufacturer's protocol. Three aliquots of Kasumi-1 cells were eletrotransfected on days 0 and 4 with *siRR* and *siMAPK1*, and in combination respectively. Kasumi-1 cells electroporated with *siMM* and mock-transfected cells were used as controls. Cell cycle analysis was performed on day 6 by FACS analysis. Briefly, cells were washed in PBS, adjusted to a cell density of 1x10^6 and fixed in 100% ice-cold ethanol for 24 h. On the next day, PBS washed cells were digested with 100 μl of RNase A for 30 min at 37˚C followed by staining with 400 μl of PI and subsequently analysed using FACSCanto II flow cytometer at 488 nm wavelength using FL3 filters with wavelength of 670 nm for the proportion cell cycle distribution in the G_0/G_1, S and G_2/M phase.

Cell viability and proliferation assays. The rate of viable cells was determined using trypan blue (Sigma-Aldrich; Merck KGaA, Darmstadt, Germany) staining method that selectively stains dead cells. Cell counting was carried out using a haemocytometer.

To quantitatively determine the number of viable cells in proliferation on days 0, 4 and 8 following electrotransfection, the *siRR*, siMAK1 and combined *siRR*/*siMAPK1*-treated Kasumi-1 cells were seeded separately, on the day of the experiment, into a 96-well plate at a density of 5x10^4/well in 100 μl complete growth medium in quadruples. Twenty microliters of 3-(4,5-dimethylthiazol-2-yl)-5-(3-carboxymethoxyphenyl)-2-(4-sulfophenyl)-2H-tetrazolium MTS/PMS solution (as instructed in the Cell Titer 96® AQueousNon-Radioactive Cell Proliferation Assay kit literature; Promega Corp., Madison, WI, USA) was added and the plate was incubated for 2 h at 37˚C in a humidified 5% CO_2 incubator. The absorbance was measured at 490 nm using an ELISA plate reader. Data are represented as mean ± SD of four independent experiments.

Microarray experiments. Post electrotransfection, genome wide expression (GWE) levels were determined in a series of four experimental conditions set up for each cell line, Kasumi-1 and SNKO-1. They include cells; co-transfected with *siRR*/*siMAPK1*; singly transfected with *siRR*; siMM; and mock-transfected cells. A total of 24 arrays, three replicates for each of the transfection experiment, were processed using Illumina HumanHT-12 v3 Expression BeadChip™ array (Illumina, San Diego, CA, USA) targeting 48,804 human transcripts per array with an average of 15-fold transcript redundancy.

Pre-hybridisation sample preparation used a total of 400-500 ng of RNA from each experiment, which was reverse transcribed to cDNA followed by amplification and *in vitro* transcription of cDNA to bio-11-dUTP-labelled complementary RNA (cRNA). Quantified (500 ng) and labelled cRNA was then hybridised to BeadChip arrays at 55˚C overnight. BeadChips were then wash-cleaned with Illumina high-stringent wash buffer. The hybridisations were scanned after staining with 1 μg/ml streptavidin-Cy3 (Amersham Biosciences, Piscatawy, NJ, USA) on the Illumina BeadArray Reader confocal scanner and BeadScan software to produce bead level data.

Background subtracted bead summary data were exported to GeneSpring™ GX 11.0 software (Agilent Technologies, Santa Clara, CA, USA) for transformation and normalisation, and differential expression analyses. Microarray expression data were normalised to the most stable three reference genes (*ACTB, B2M* and *UBC*). Probe sets returning a P-value <0.05 (unpaired t-test) in comparison to the mock cells and experiment classes were considered to be differentially expressed. The differentially expressed genes were then filtered for gene sets that had fold-changes >1.1, and >1.5 together with false discovery rate (FDR) adjusted P-value ≤0.05.

The processed data were used for GO annotation and KEGG pathway enrichment analyses using the Database

for Annotation, Visualization and Integrated Discovery [DAVID; (22)].

Statistical analysis. All statistical analysis was performed using SPSS software version 17 (SPSS, Inc., Chicago, IL, USA). Paired t-test was used to measure mean differences between two variables whereas one-way ANOVA was used to measure mean differences between three variables.

Results

siRNA induces the silencing of RUNX1-RUNX1T1 and MAPK1 in Kasumi-1 cells. To identify the silencing efficacies of *siMAPK1* and *siRR*, we transfected Kasumi-1 cells with 100 and 200 nM of the respective siRNAs separately in triplicates. Time course suppression of *RR* and *MAPK1* genes in the experimental cells were compared with mock-transfected cells. The results of qRT-PCR showed that *siMAPK1* inhibited the expression of *MAPK1* by 85% on day one, and lasted for at least three days with 2% recovery (83%) on day two and 6% recovery (77%) on day three (Fig. 1A). *siRR*-treated Kasumi-1 cells exhibited up to 78% suppression of *RR* expression at 24 h and continued to further suppress to 82% at 48 h before 16% recovery was observed at 72 h. These observations as measured by qRT-PCR validates that significant knockdown (>80%) of *RR* and *MAPK1* was achieved with respective doses of 200 nM of *siRR* and 100 nM of *siMAPK1* at 48 h post-transfection. Melting curves for RUNX1-RUNX1T1 and MAPK1 are included in Fig. 1B and C, respectively.

Whole genome expression profile. We conducted gene expression analysis on mRNA extracts obtained at 48 h post-transfection using Illumina's HumanHT-12 v3 Expression BeadChips. A total of 24 arrays, three replicates for each of the four experimental conditions for both Kasumi-1 and SKNO-1 cells (as described above) were profiled for at least 48,804 transcripts to characterise the genes modulated when *RR* and *MAPK1* were downregulated.

Microarray data for Kasumi-1 cells co-transfected with *siMARK1* and *siRR* showed a total of 4,788 differentially expressed genes (DEG) as compared to the mock cells, accounting for 9.8% of the transcriptome probed in our array. However, when the 4,788 DEGs were conditioned to a fold change (FC) ≥1.5 and P<0.05 (t-test), the gene set condensed to 466 representing 262 upregulations and 204 downregulations. Relative to Kasumi-1 cells, co-knockdown of *RR* and *MAPK1* genes in SKNO-1 cells revealed a more pronounced gene modulation presenting with 6,465 DEGs accounting for 13.2% of the transcriptome studied. Of these 6,465 DEGs, 732 sequences had a FC of ≥1.5 (at P<0.05) representing 415 upregulations and 317 downregulations.

We then examined the 466 and 732 gene sets with FC >1.5 for shared common genes modulated in both Kasumi-1 and SKNO-1 cells using the two-way Venn diagram analysis. In total, there were 148 overlapping genes, which included 109 upregulations and 39 downregulations (Fig. 2A). We also looked at the shared genes between the two cell lines when the fold changes were relaxed to 1.1. At this fold change, we observed 4,855 and 4,974 genes that were modulated in their respective co-transfected Kasumi-1 and SKNO-1 cell lines when compared to their respective mock-transfected cells. When used on two-way Venn diagram, these two enriched gene sets presented with 884 overlapping genes, which included 478 upregulations and 406 downregulations (Fig. 2B).

Whole genome expression studies from isolated *RR*-depleted Kasumi-1 cells presented with 5,178 DEGs relative to mock-transfected cells, accounting for 10.6% of the transcriptome probed. One-tenth of these, 552 genes, had a fold change expression ≥1.5 including 300 upregulations and 252 downregulations. In turn, *RR*-depleted SKNO-1 altered the expression of 9,049 genes. Of these, expression of 2,600 genes was significantly changed at a ≥1.5-fold cut-off including 1,267 upregulations and 1,333 downregulations. Two-way Venn diagram analysis enrolling the gene sets observed at fold changes ≥1.5 from Kasumi-1 cells (552) and SKNO-1 cells (2,600) revealed that a subset of 284 DEGs (including 197 upregulations and 87 downregulations) were common between the two cell lines (Fig. 2C), and support their association with the *RR* knockdown. Moreover, when the absolute fold change cut-off was adjusted to ≥1.1, we observed the number of overlapping genes from the two cell lines rose to 1,891, with 971 upregulations and 920 downregulations (Fig. 2D).

Gene ontology analysis. To reveal the potential function of differentially expressed genes common for both Kasumi-1 and SKNO-1 cell lines in terms of their associated biological processes, cellular components and molecular functions, we used the online data-mining tools of DAVID software (23,24). Uploading the 148 overlapping gene set, derived from the *siRR* + siMAPK experiment as depicted on the Venn diagram Fig. 2A, into DAVID with the default gene ontology (GO) setting (P<0.01) indicated association to 267 biological processes (BP), 49 cellular components (CC) and 52 molecular functions (MF). GO enrichment analysis for the 284 overlapping gene set identified from the Venn diagram analysis (Fig. 2C) from *siRR* experiments on Kasumi-1 and SKNO-1 cell lines identified 269 BP, 85 CC and 69 MF.

qRT-PCR validation of microarray data. In order to validate the altered gene expression results of the BeadChip experiments, we performed quantitative PCR following reverse transcription (qRT-PCR) on the same RNA isolates used on BeadChips. We chose to quantify the expression levels of *MAPK1* and *RR*, and compared the fold changes.

qRT-PCR assessment of *RR* and *MAPK1* gene expression levels from the co-transfection experiment showed comparable downregulated fold changes validating the microarray data. As illustrated in Fig. 3, *RR* expression in co-transfected Kasumi-1 and SKNO-1 cells revealed a fold change between 1.75-1.85 and 1.4-1.6, respectively on qRT-PCR, while the same on the BeadChip had fold change downregulations between 2.4-2.6 and 1.9-2.3, respectively. Similar agreements were observed for *MAPK1* in the co-transfected experiments. *MAPK1* had a downregulated fold changes between 2.4-2.6 and 2.6-3.0 by qRT-PCR and 3.8-3.9 and 2.8-3.6 by BeadChip in Kasumi-1 and SKNO-1 cells, respectively.

The results from the isolated *RR* knockdown experiment were also consitent with those of BeadChip. On a log2 scale, qRT-PCR revealed that *RR* expression was downregulated

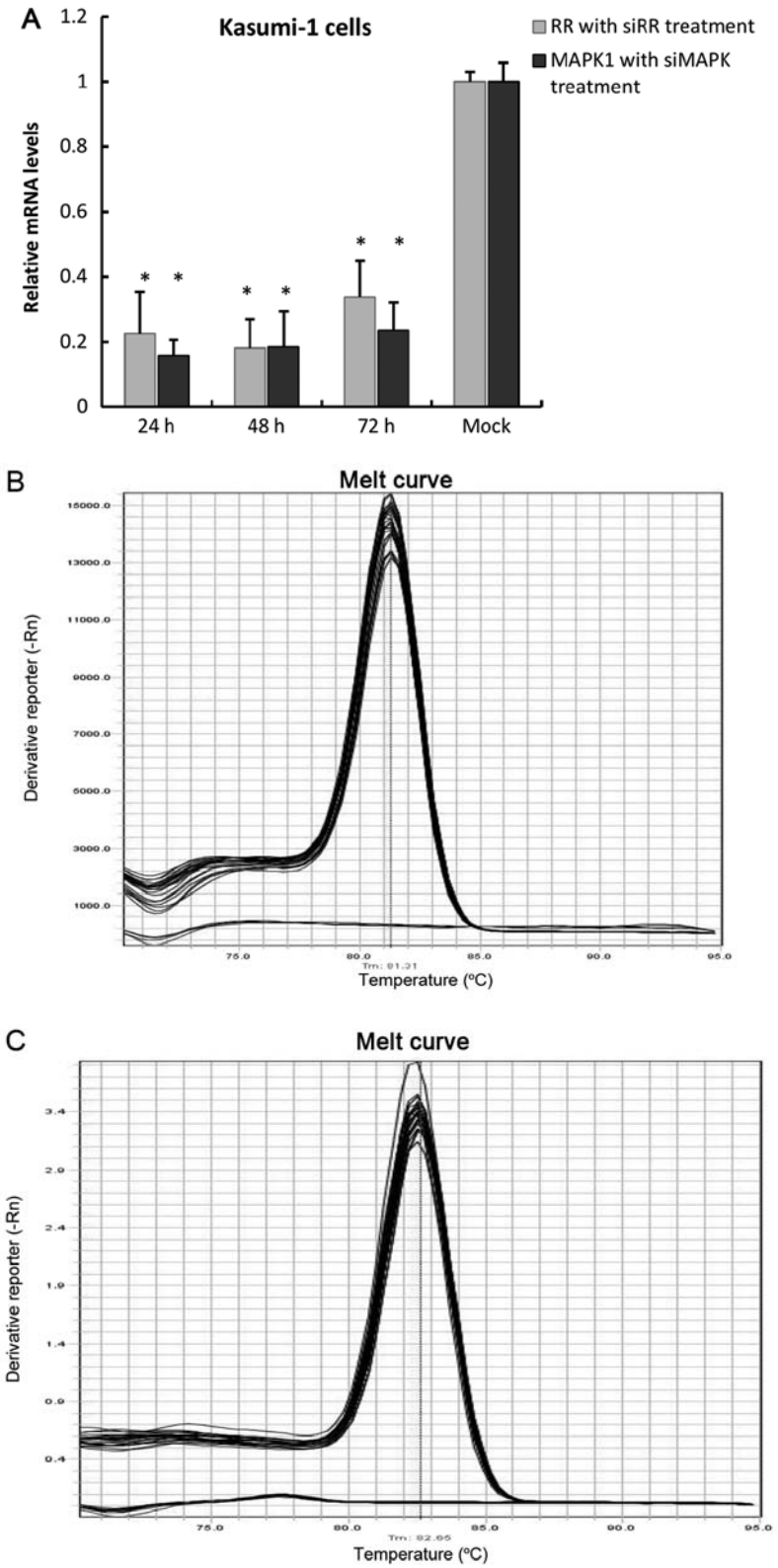

Figure 1. (A) Time-course depletion effect of the target mRNA concentration assessed using qRT-PCR at 24, 48 and 72 h after single transfection of Kasumi-1 cells with 100 nM of *siMAPK1* and 200 nM of *siRR*. Reductions in *MAPK1* and *RR* transcripts at three time points are shown. The mean values with error bars to indicate standard deviations were calculated from three independent experiments. Student's t-test was performed on each data set relative to mock data (*P<0.05). (B) Melt curve analysis of AML/ETO (RR). A single peak is observed at T_M 81.31. (C) Melt curve analysis of MAPK1. A single peak is observed at T_M 82.65. AML, acute myeloid leukaemia. siMAPK1, siRNA-MAPK1; siRR, siRNA-RUNX1-RUNX1T1.

by 1.5-1.7- and 1.6-1.7-fold, while the same on microarray was 2.9-3.3 and 3.2-3.7 in Kasumi-1 and SKNO-1 cells, respectively.

RUNX1-RUNX1T1 and MAPK1 suppression reduces the proliferation rate of t(8;21) cells. To determine the effect of *RUNX1-RUNX1T1* and *MAPK1* suppression and their

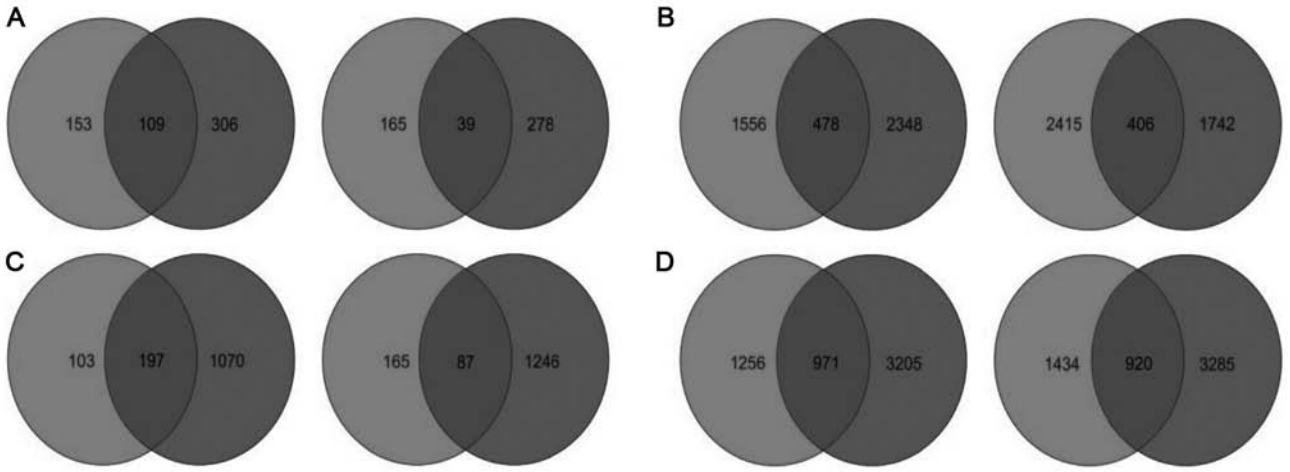

Figure 2. The two-way Venn-diagrams display the total number of unique and overlapping gene expression changes as a result of *RR* and *MAPK1* gene supression in Kasumi-1 cells (dark grey circles) and SKNO-1 cells (light grey circles). (A) Two-way Venn diagram shows the number of shared 109 upregulated (left) and 39 downregulated (right) gene changes between cell lines co-transfected with *siRR* and *siMAPK1* when absolute fold change was set for 1.5 with P≤0.05 by one-way ANOVA. (B) Similar to A but with the fold changes relaxed to 1.1. (C) Venn diagram shows the number of shared upregulated (left) and downregulated (right) gene changes between cell lines singly transfected with *siRR* with absolute fold change set for 1.5 with P≤0.05 by one-way ANOVA. (D) Similar to C with fold change adjusted to 1.1. siMAPK1, siRNA-MAPK1; siRR, siRNA-RUNX1-RUNX1T1.

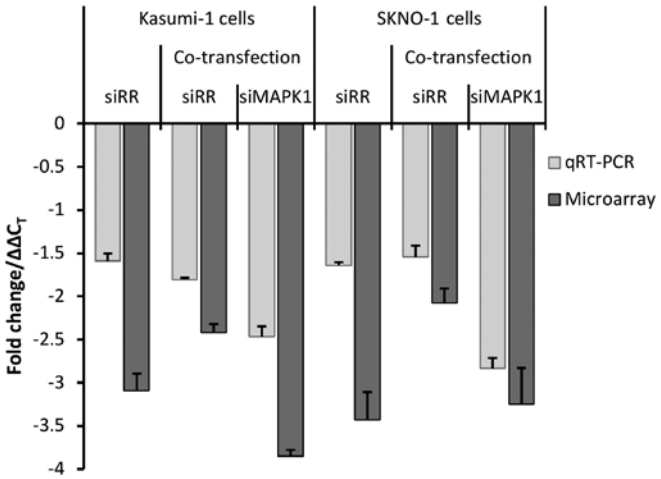

Figure 3. Validation of microarray data for Kasumi-1 and SKNO-1 cell lines by qRT-PCR. Microarray signal intensity and qRT-PCR *MAPK1* and *RUNX1-RUNX1T1* mRNA copy number were determined in triplicates, normalised to *B2M* expression and reported as means with error bars to indicate standard deviations. siMAPK1, siRNA-MAPK1; siRR, siRNA-RUNX1-RUNX1T1.

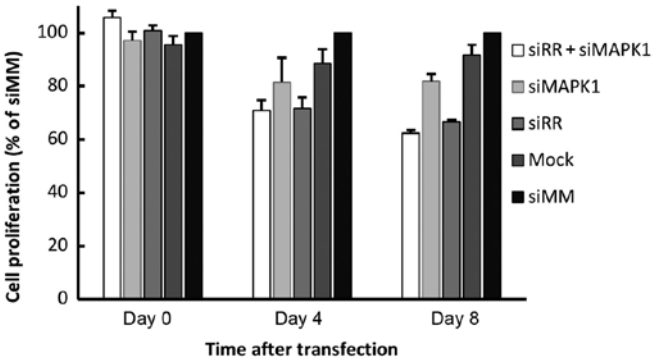

Figure 4. Effect of each siRNA on the suppression of cell proliferation. MTS assays on days 0, 4 and 8 show the time course inhibition of proliferation of Kasumi-1 cells upon knockdown of *MAPK1* and *RUNX1-RUNX1*. Error bars indicate standard deviations of two independent experiments. All experiments were carried out in four replicates. siMM, scrambled mismatch siRNA; siMAPK1, siRNA-MAPK1; siRR, siRNA-RUNX1-RUNX1T1.

combined influence on the proliferation rate, we transfected Kasumi-1 cells three successive times in a gap of three days with their respective siRNAs individually and in combination. MTS assays were performed on days 0, 4 and 8 to determine the proliferation activity. siMM and mock-transfected Kasumi-1 cells served as controls.

We observed that a single co-transfection with *siRR* and *siMAPK1* or isolated transfection of *siRR* was not sufficient to inhibit the proliferation of Kasumi-1 cells when compared with siMM (Fig. 4). However, sequential electroporations on every third or fourth day attenuated the proliferation viabilities on days 4 and 8 in both the experiments. Similarly, two successive transfections of *siMAPK1* were required to inhibit Kasumi-1 cell proliferation by 18.5% on day 4. The third successive transfection was only sufficient to sustain the proliferation at the same level on day 8. These data suggest that the fusion protein RR plays a more substantial role than MAPK1 in supporting the proliferation of leukaemic cells with t(8;21).

Our GO enrichment analysis revealed that the observed growth suppression upon *RR* knockdown was accompanied by deregulated expression of classical positive regulator genes that otherwise are known to enhance cell proliferation. They include significant downregulation of *FLT3, HIF1A, KIT, MYCN, LYN, UBE2A, TBRG4, RPS9, RPS15A, RPA1, PRDX3, PDF, ODC1, IL13RA1, ITGB1, GRN, FABP1, CDK6, F2R, CDC123, CAPNS1, MARCKSL1, CD40, BCL2L1, AGPAT1, MXI1, CAV2, ENG, EMP3, IL8, MFN2* and *TRIM24* genes, and upregulation of *CEBPA, S100A11, ING4* and *SSTR2* genes. On comparison, GO enrichment analysis for category of proliferation from *RR* knockdown and *RR/MAPK1* co-knockdown experiments revealed several shared differentially expressed genes. On exclusion of the simultaneously altered genes, we

Table I. Summary of Gene Ontology Enrichment Analysis according to pathways indicated when genes were silenced using the respective siRNAs.

Pathways	*RUNX1-RUNX1T1* (siRR)	*MAPK1* (siMAPK1)
Cell proliferation	Upregulated genes	Upregulated genes
	CEBPA	*VHL*
	S100A11	*ZBTB16*
	ING4	*BTG1*
	SSTR2	
	Downregulated genes	Downregulated genes
	FLT3	*FLT3*
	HIF1A	*NRAS*
	KIT	*STAT1*
	MYCN	
	LYN	
	UBE2A	
	TBRG4	
	PRDX3	
	CD40	
	IL8	
	BCL2L1	
Apoptosis	Upregulated genes	Upregulated genes
	BCL2	*TP53*
	SPHK2	*TNFSF10*
	CFLAR	*ADA*
	CD24	
	NOTCH1	
	ADAM17	
	BIRC3	
	HMGB1	
	Downregulated genes	Downregulated genes
	IP6K2	*JUN*
	BECN1	*NRAS*
Differentiation	Upregulated genes	Upregulated genes
	CD24	*ADA*
	NOTCH1	
	DNMT38	
	CEBPA	
	CEBPE	
	ID2	
	JMJD6	
	IK2F1	
	Downregulated genes	Downregulated genes
	RHOA	*JUN*
	CBFB	
	KIT	
	CDK6	
	FLT3	
Cell cycle	Upregulated genes	Upregulated genes
	FOXO4	*RASSF1*
	ING4	*GADD45A*
		p53
		FBX06
	Downregulated genes	Downregulated genes
	TPX2	*MAPK11*
	CDC2	
	CKAP5	
	IL8	
	MAD21L	
	CCNE2	
	CCNG2	
	CDK6	
	TBRG4	

siMAPK1, siRNA-MAPK1; siRR, siRNA-RUNX1-RUNX1T1.

observed that downregulation of *JUN*, *NRAS*, and *STAT1* genes and upregulation of *VHL*, *ZBTB16* and *BTG1* genes were unique to *MAPK1* depletion. The results of the GO enrichment analysis are summarised in Table I.

RUNX1-RUNX1T1 suppression exerts an anti-apoptotic effect while MAPK1 suppression induces apopotosis in t(8;21) cells. Next, we examined the consequences of isolated and co-depletions of *RR* and *MAPK1* on cell apoptosis. Kasumi-1 cells harvested on day 9, after three consecutive transfections, were double stained using Annexin V/FITC and PI.

Three consecutive *siRR* treatments significantly (P=0.0001) lowered the live cells by 24% when compared with the siMM control indicating that *RUNX1-RUNX1T1* suppression has an apoptotic effect on Kasumi-1 cells (Fig. 5). Notably, pronounced apoptosis (30±1.6%) was observed upon isolated *MAPK1* deletion, and revealed a significant difference (P<0.0001) when compared with control cells. However, co-depeletion demonstrated no difference when compared with the siMM control cells. FACS results for the apoptosis analysis are shown in Fig. 5B-E.

GO enrichment analysis on shared DEGs from both Kasumi-1 and SKNO-1 cells with fold change of ≥1.5 in response to RR depletion exhibited several changes to genes involved in negative regulation of apoptosis. They included significant upregulation of *BCL2*, *SPHK2*, *CFLAR*, *CD24*, *NOTCH1*, *ADAM17*, *BIRC3* and *HMGB1*, and downregulation of *IP6K2* and *BECN1* genes. Exclusion of overlapping differentially expressed genes involved in apoptosis between the isolated RR knockdown and the co-knockdown experiments revealed five genes specific for *MAPK1* depletion. They include upregulated expression of *TP53*, *TNFSF10* and *ADA* genes as well as downregulated expression of *JUN* and

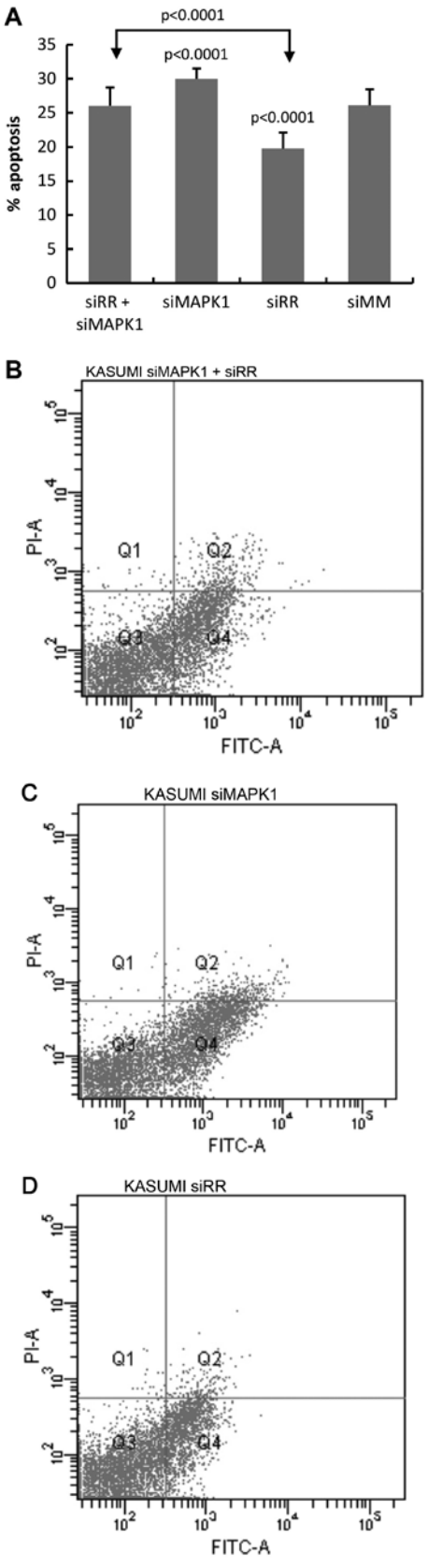

Figure 5. (A) Histogram represents the knockdown effects of *MAPK1*, *RUNX1-RUNX1T1* and their combined suppression on apoptosis induction in Kasumi-1 cells. Error bars indicate standard deviations of two independent experiments each with triplicate technical replicates. P-value of silenced genes vs. control siRNA was determined by one way ANOVA. (B) FACS results of apoptosis induction by co-knockdown of MAPK1 and *RUNX1-RUNX1T1* (siMAPK1 + siRR). (C) FACS results of apoptosis induction by knockdown of MAPK1 (siMAPK1). (D) FACS results of apoptosis induction by knockdown of *RUNX1-RUNX1T1* (siRR).

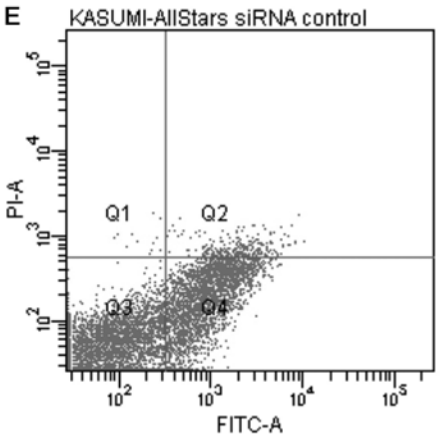

Figure 5. Continued. (E) FACS results of apoptosis induction by knockdown with negative control siRNA (siMM).

NRAS genes. The results of the GO enrichment analysis are summarised in Table I.

RUNX1-RUNX1T1 suppression supports, while MAPK1 depletion inhibits the differentiation of t(8;21) cells. To investigate the effect of *RUNX1-RUNX1T1* and *MAPK1* depletion on the progenitor status of Kasumi-1 cells, we analysed the CD34 expression levels as an indicator of differentiation. Compared with the cells, *RR* suppression showed statistically significant (P=0.0001) loss of CD34-expressing cells by ~23±1.1% 9 days after the first of the three successive electroporations indicating that the cells were undergoing apparent differentiation (Fig. 6A). The loss of CD34-expressing cells corresponded with an increase in cells expressing CD45 which indicated differentiation. The FACS results are shown in Fig. 6B-E, respectively. Based on the gene ontology analysis on the RR-suppressed microarray data, we identified several genes involved in cell differentiation to be activated or repressed. Upregulated genes included *CD24, NOTCH1, DNMT3B, CEBPA, CEBPE, ID2, JMJD6* and *IKZF1*, while *RHOA, CBFB, KIT, CDK6* and *FLT3* were downregulated.

When both *MAPK1* and *RR* were co-suppressed, the expression of CD34 in Kasumi-1 cells were relatively less pronounced (13±2.3%) (Fig. 6A). However, CD34 suppression revealed a significant difference (23±1.1%), when compared with the control cell expression in which only RR was suppressed. This implies that *MAPK1* abrogated the effect of *RR* by ~40% suggesting that tandem *MAPK1* suppression exerted an anti-differentiation effect. Due to this antagonist effect of *MAPK1* and *RR* co-suppression, we used the same strategy mentioned in the apoptosis section to identify the genes more specific for *MAPK1* knockdown. After exclusion, *MAPK1* knockdown revealed significant downregulation of c-*JUN* and upregulation of *ADA*, both identified to have anti-differentiation effect.

FACS experiment on isolated *MAPK1* suppression showed no significant loss of CD34 expression when compared with mock and AllStar siRNA-treated control cells (Fig. 6A). The results of the GO enrichment analysis are summarised in Table I.

RUNX1-RUNX1T1 and MAPK1 depletion promotes cell cycle arrest. Finally, we examined the effect of different siRNAs on

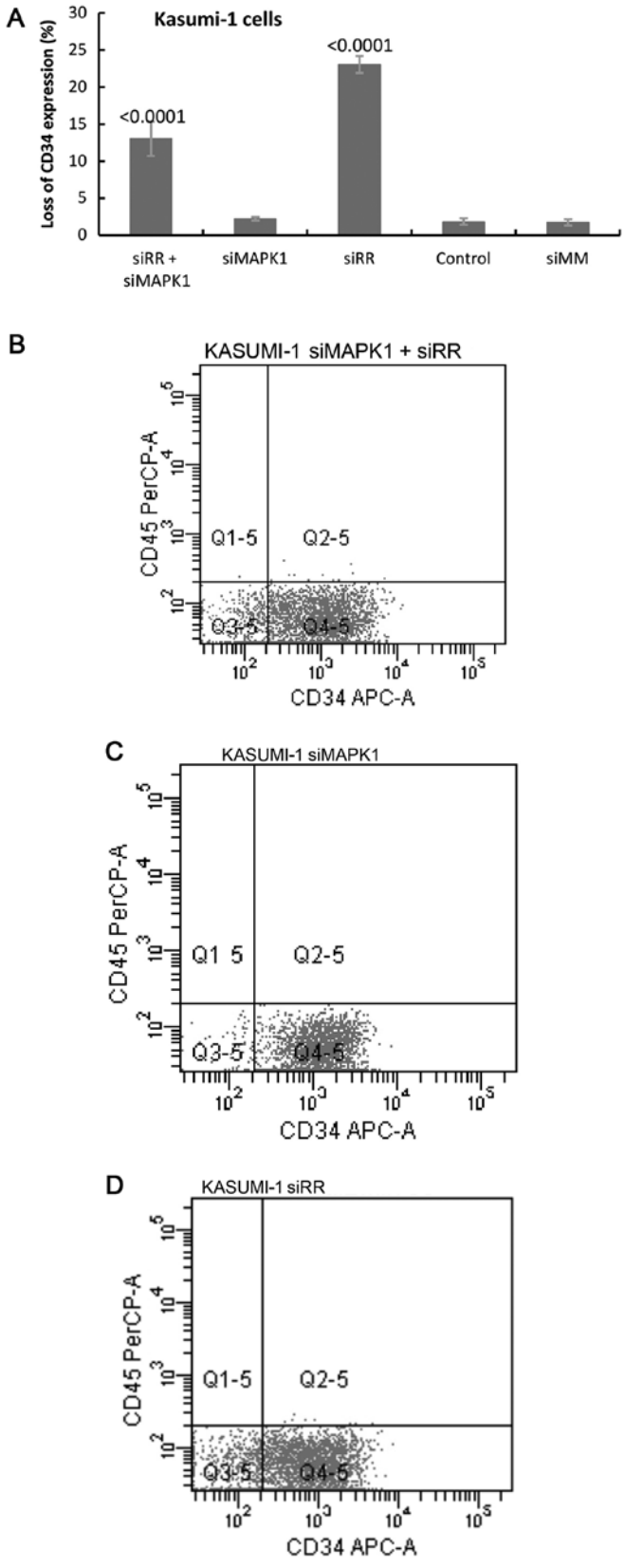

Figure 6. (A) Effects of *MAPK1*, *RUNX1-RUNX1T1* and combination of *MAPK1* and RUNX1-RUNX1T1 suppression on differentiation induction/suppression. Error bars indicate standard deviations of two independent experiments each with triplicate technical replicates. P-value of silenced genes vs. mock control was determined by one way ANOVA. (B) FACS results of differentiation induction/suppression by co-knockdown of MAPK1 and *RUNX1-RUNX1T1* (siMAPK1 + siRR). (C) FACS results of differentiation induction/suppression by knockdown of MAPK1 (siMAPK1). (D) FACS results of differentiation induction/suppression by knockdown of *RUNX1-RUNX1T1* (siRR).

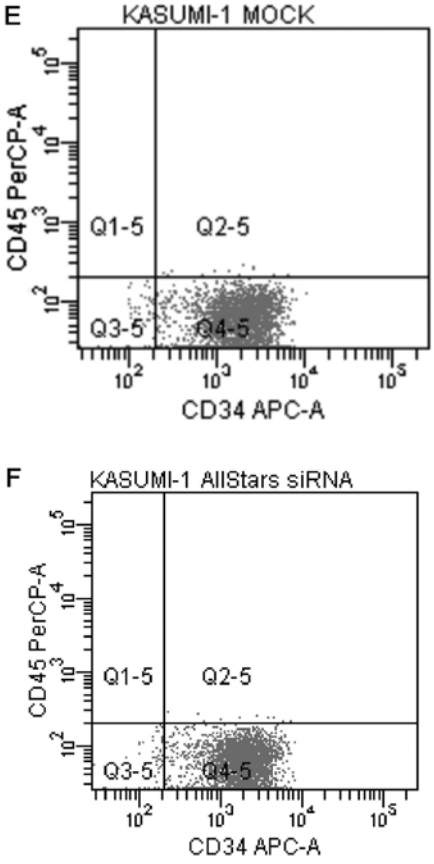

Figure 6. Continued. (E) FACS results of differentiation induction/suppression by Kasumi-1 cells without siRNA (Mock). (F) FACS results of differentiation induction by knockdown with negative control siRNA (siMM).

cell cycle progression. Kasumi-1 cells were electro-transfected twice o a gap of three days with either *siRR*, *siMAPK1* or co-transfected with *siRR*/*siMAPK1*. Cell phase distributions were analysed on day 6 by flow cytometry. In comparison with the mock-transfected cells, *RR* suppression showed a reduction in the percentage of cells in the S and G2M phases (Fig. 7A). This was correlated with increased cells in the G_0/G_1 phase by ~13%. Gene expression data following *RR* depletion in the Kasumi-1 and SKNO-1 cell lines showed that several genes involved in positive and negative regulation of the cell cycle were variably expressed. Upregulated genes included *FOXO4* and *ING4*, and downregulated genes were *TPX2*, *CDC2*, *CKAP5*, *IL8*, *MAD2L1*, *CCNE2*, *CCNG2*, *CDK6*, *TBRG4* and *KPNA2*. Isolated *MAPK1* suppression also caused an increased growth arrest. This was accompanied with reduction in G2M and S phases, while cells in the G_0/G_1 phase were increased (Fig. 7A). FACS results for the cell cycle analysis are included in Fig. 7B-F, respectively.

Combined targeting of *RR* and *MAPK1* yielded further reduction of cells in S and in G2M phase by ~40 and 70%, respectively, when compared to the mock cells. This also led to an increased number of cells in the G_0/G_1 phase by ~25%. Gene ontology for double knockdown of *RR* and *MAPK1*, after exclusion of common target genes, demonstrated that several protein coding genes were uniquely responsive to the depletion of *MAPK1*; they included upregulation of *RASSF1*, *GADD45A*, *P53* and *FBXO6*, and downregulation of *MAPK11*. The results of the GO enrichment analysis are summarised in Table I.

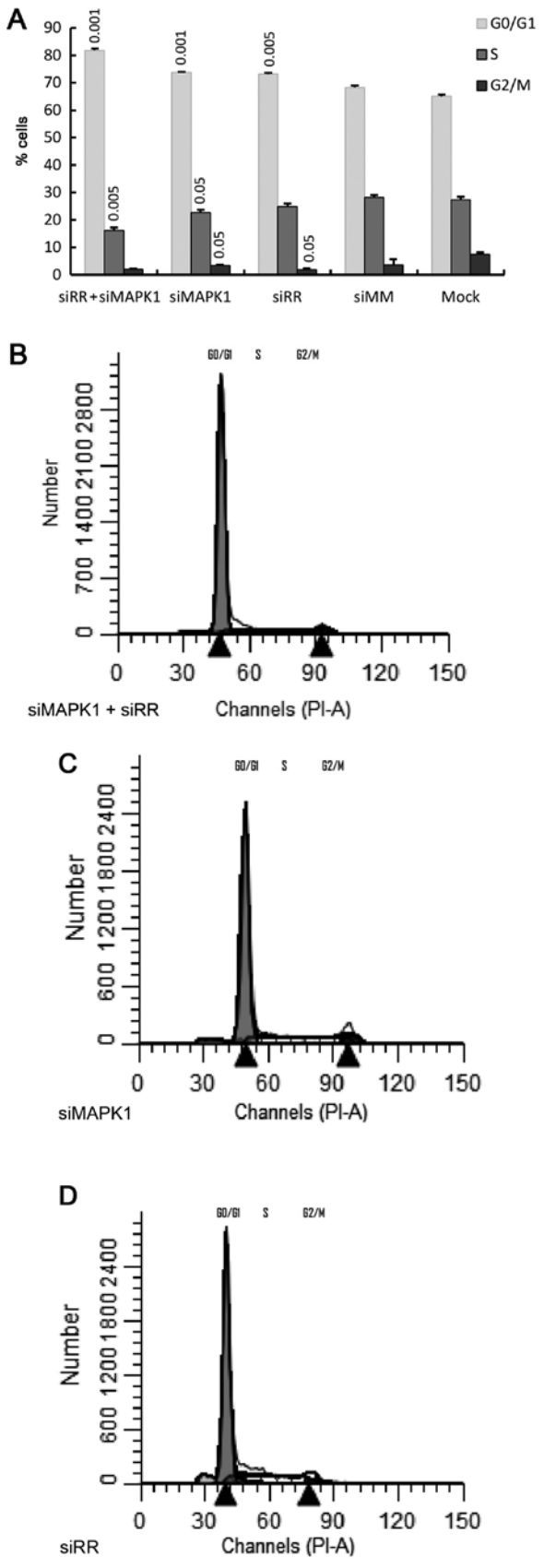

Figure 7. (A) *MAPK1, RUNX1-RUNX1T1* and their co-suppressions induces growth arrest. Error bars indicate standard deviations of two independent experiments. P-value of silenced genes vs. mock control was determined by one way ANOVA. (B) FACS results of cell cycle shifts induced by co-knockdown of *MAPK1* and *RUNX1-RUNX1T1* (siMAPK1 + siRR). (C) FACS results of cell cycle shifts induced by knockdown of MAPK1 (siMAPK1). (D) FACS results of cell cycle shifts induced by knockdown of *RUNX1-RUNX1T1* (siRR).

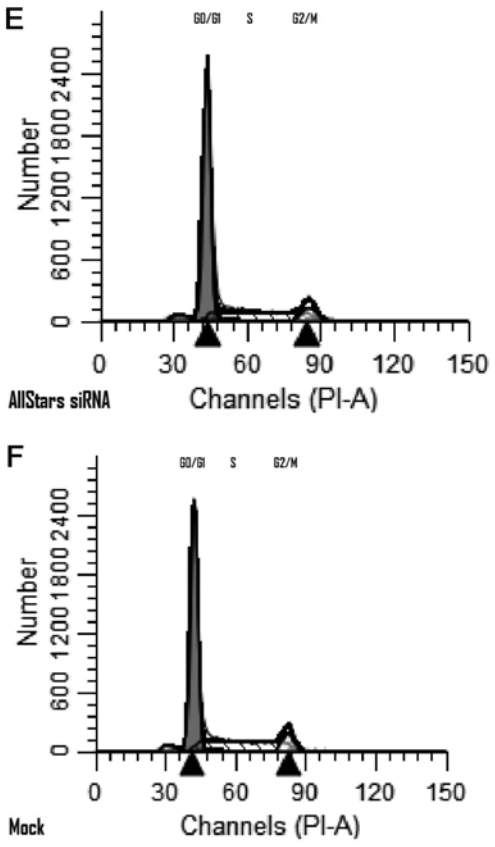

Figure 7. Continued. (E) FACS results of cell cycle shifts induced by knockdown with negative control siRNA (siMM). (F) FACS results of cell cycle shifts induced by Kasumi-1 cells without siRNA (Mock).

Discussion

The consequence of *RR* translocation in haematopoietic precursors is characterised by clonal proliferation with reduced capacity to differentiate into committed progenitors and therefore functional myeloid cells. Although the primary genetic aberration t(8;21) found in self-renewing malignant haematopoietic stem cells significantly alters the regulatory processes controlling the growth and differentiation programmes, an associated secondary lesion is often essential for the leukaemic transformation and maintenance. Taken together, both primary and secondary lesions confer a proliferation advantage and impair haematopoietic differentiation in AML. Deregulated signalling in the RAS/RAF/MEK/ERK pathway has often been implicated with leukaemia, particularly in the RAS-RAF node of the pathway (25,26). In this study, our focus was to identify the patterns and networks of genes that were either upregulated or downregulated driving the tumourigenic processes including proliferation, apoptosis, cell cycle and differentiation when *RR* and *MAPK1* were suppressed. Gene expression profiling has played a key role in providing us with important clues to these processes.

We showed that continuous suppression of *RR* is important for inhibiting cell proliferation, a finding extensively validated and characterised by many researchers (21,27). Our GO enrichment analysis showed that this dampened proliferation was largely due to the downregulation of several genes that are otherwise known to enhance cell proliferation. Most

important among them were *KIT* and *FLT3* genes that encode to class III transmembrane receptor tyrosine kinases (RTK), which play a crucial role in haematopoiesis. While the expression of *FLT3* in haematopoietic stem cells and progenitors are important to maintain cell survival (28), *c-Kit* expression by myeloblasts observed in ~80% of patients with AML typically enhances proliferation (29). A negative correlation between the level of *c-Kit* expression intensity on myeloblasts and the number of leukocytes in the blood of AML patients has been reported suggesting its role in myeloblast egression into peripheral circulation (30). As these RTKs are immediately upstream of the Ras/RAF/MAPK/ERK pathway, their constitutive activation may lead to aberrant signalling, proliferation and differentiation. Leveraging on this abnormal signalling mechanism, several small-molecule tyrosine kinase inhibitors have been developed and investigated as potential FLT3- and c-KIT-targeted therapies for RTKs expressed on myeloblasts in AML. It appears that patients with AML benefit from a synergistic approach of kinase inhibitors used in combination with conventional chemotherapy in controlling proliferation (31). On further dissection, the same set of genes involved in inhibiting proliferation is also involved in other biological processes. Based on the functional and biological connectivity analysis on shared DEGs between cell lines in response to RR suppression, at least eight (*HIF1A, ITGB1, BCL2L1, CDK6, CEBPA, IL8, FLT3 and KIT*) DEGs were involved in cancer pathways, five genes (*IL13RA1*, *CD40*, *KIT*, *FLT3* and *IL8*) in cytokine-cytokine receptor interactions and three genes (*CEBPA, KIT* and *FLT3*) in the AML pathway.

We also showed that the antiproliferative consequence of the co-suppression of *MAPK1* and *RR* was biologically no different from the effect exerted by isolated repression of *RR* in Kasumi-1 cells. This failure of *MAPK1* depletion to augment the level of the antiproliferation effect resulting from *RR* suppression suggests the lack of coordinative synergy between the DEG sets. Thus delivery of MAPK1 with RR siRNA may not serve as an attractive gene therapy modality to control abnormal proliferation in t(8;21) AML cells. GO enrichment analysis of the BeadChip data from the *MAPK1* suppressed Kasumi-1 and SKNO-1 cell lines demonstrated six (6) DEGs with the biological process of regulating cell proliferation. Among them, we found that the expression of the *NRAS* oncogene (an upstream GTPase in the classical ERK pathway) was suppressed in a *MAPK-1*-dependent manner illustrating a possible feedback loop within the ERK pathway. A previous study reported that ERK exerts a negative feedback by interfering with RAS activation by phosphorylating son of sevenless (*SOS*), an immediate early gene in the ERK cascade (32). Another interesting target of *MAPK1* associated with the proliferation and apoptosis in Kasumi-1 cells was the transcription factor *JUN*, a subunit of the activator protein-1 (AP-1) important for transactivation of *CDKN2D*. Downregulated expression of *JUN*, in the absence of *MAPK1* suggests a cross-talk between the ERK and JNK pathways. A similar observation has been made where *ERK* and Jun kinases underlie the vascular endothelial cell growth factor-induced proliferation in endothelial cells (33). These observations suggest that *MAPK1*, the terminal kinase in the ERK signalling pathway, may play a less significant role in the progression of AML cells, and could be less effective as a druggable target than *RR* in terms of impeding cell proliferation. Another target of MAPK1 was the downregulation of *ZBTB16*, a transcription factor that regulates the expression of genes involved in cell growth and apoptosis, and may have complemented the reduced proliferation observed in our study.

This study identified a panel of 10 genes whose differential expression exerted an anti-apoptotic effect on leukaemic myeloblast secondary to selective RR silencing. These identified included upregulated *BCL2*, *SPHK2*, *CFLAR*, *CD24*, *NOTCH1*, *ADAM17*, *BIRC3* and *HMGB1*, and downregulated *IP6K2* and *BECN1* genes. More important were the overexpression of anti-apoptotic *BCL2*, *BIRC3* and *CFLAR* genes. Studies have shown that enhanced expression of *BCL2* in leukaemic myeloblasts offers them a survival advantage by regulating the release of apoptogenic proteins from mitochondria, notably cytochrome *c*, and resistance to chemotherapy (34,35). This anti-apoptotic characteristic is further strengthened by the increased activity of BIRC3, a member of the IAP family of proteins, that acts as endogenous inhibitor of caspases (36). Furthermore, the loss of *RR* caused increased expression of *CFLAR*, a critical anti-apoptotic regulator of apoptosis.

Although the selective *RR* silencing inflicts an anti-apoptotic phenotype in t(8;21) myeloblasts, *MAPK1* suppression reciprocally induces apoptosis while their co-suppression ameliorates the effect (Fig. 5). This relative refractory survival of t(8;21)-positive blasts upon enforced silencing of *MAPK1* may be due to the apoptotic mitochondrial changes stimulated by the activity of upregulated *TP53* and *TNFSF10*, and downregulated *JUN* gene, which regulates the release of cytochrome *c* and drives the proteolytic caspases. Additionally, *NRAS* and *JUN*, members of the classical MAP kinase and *JNK* pathways, respectively, were downregulated following the treatment of siMAPK1, demonstrating a link between the two pathways. It was previously shown that oncogenic *RAS* activates c-*JUN* via a separate pathway from the activation of extracellular signal-regulated kinases (37).

The significant loss of CD34 expression in the RR-suppressed cells suggested that the fusion gene expression exerted an anti-differentiation effect. Biological analysis revealed that 13 genes, in response to RR suppression, were involved in driving this process, and among them at least eight genes (*CEBPA*, *CEBPE*, *ID2*, *JMJD6* and *IKZF1*, *CBFB*, *KIT* and *CDK6*) were directly responsible for myeloid progenitor cell differentiation. Both *CEBPA* (CCAAT enhancer binding protein α) and *CEPBE* are myeloid-specific transcription factors that function as crucial regulators of granulopoiesis. Their respective knockout mice have shown to block the differentiation of common myeloid progenitor cells into granulocyte-macrophage progenitor cells accompanied by granulocytopaenia (38,39). Apart from its role in differentiation, the consistent upregulation of myeloid transcription factor CEBPA has been shown to arrests t(8;21) AML cell proliferation through direct inhibition of CDK2 and CDK4 (40). A similar mechanism may be partly responsible for reduced proliferation in our study as *RR* knockdown resulted in upregulation of *CEBPA* and downregulation of the G_1 kinase CDK6, the homolog of CDK4. The observed increased expression of *ID2* subsequent to RR suppression may function at later stages of differentiation of t(8;21) to silence myeloblasts. This conclusion is proposed as

previous research has shown that *ID2* mRNA is constitutively expressed in more mature myeloid blast cells and the level markedly increased towards terminal myeloid differentiation (41). Notably, we observed that *CBFB*, which is required for myeloid and lymphoid differentiation, was downregulated with the suppression of *RR* suggesting that its deficiency does not block the differentiation of myeloid progenitors. The observed loss of CD34 expression is further intensified by the downregulation of *CDK6* which otherwise is known to block myeloid differentiation by interfering with RUNX1 DNA binding and RUNX1-C/EBPα interaction (42).

Knockdown of *MAPK1*, but not *RR*, exhibited elevated expression of *ADA* and downregulation of *JUN*; both of which have been known to confer anti-differentiation effects (43). Therefore, it is not surprising that *MAPK1*-mediated differential expression of *ADA* and *JUN* did not alter the differentiation characteristics of the AML blasts (Fig. 6).

We showed that reduced proliferation upon isolated *RR* and *MAPK1* depletion was paralleled by cell cycle arrest at the G_0/G_1 phase. A tightly regulated molecular mechanism that controls the accurate transition from G_1 phase of the cell cycle to S phase is crucial for eukaryotic cell proliferation, and its de-regulation promotes oncogenesis. Upon siRNA-mediated RR depletion, we showed that eight genes (*TBRG4*, *CCNE2*, *FOXO4*, *CDK6*, *ING4*, *IL8*, *MAD2L1* and *CCNG2*) under the GO category of negative regulation of the cell cycle were downregulated except *FOXO4*. Noteworthy is that the accumulation of Kasumi-1 cells in the G_1 phase of the cell cycle in response to RR suppression was important due to the combined downregulated expression of *CDK6* and *CCNE2* (cyclin E2). Regulatory protein CDK6 is a catalytic subunit of the protein kinase complex that is important for cell cycle G_1 phase progression and G_1/S transition. GO enrichment analysis shows that the observed G_1 arrest in response to *MAPK1* depletion in t(8;21) myeloblasts was the result of increased expression of negative regulators of the cell cycle: *RASSF1*, *FBXO6*, *DADD45A* and *P53*. RASSF1A is an important human tumour-suppressor protein that inhibits the accumulation of cyclin D1 and induces cell cycle arrest acting at the level of G_1/S phase cell cycle progression by engaging the Rb protein family (44). GADD45α-induced cell cycle arrest leads to a reduced cell proliferation rate. This is achieved by its interaction with cyclin-dependent kinase inhibitor $p21^{waf/cip/mda-6}$ leading to cell cycle arrest at G_1/S transition due to disruption in the formation of a CDK/cyclin complex (45). Most importantly, depletion of *MAPK1* significantly increased the expression of P53 and leads to cell cycle arrest and apoptosis as observed in this study.

The present study primarily utilised siRNAs to silence target genes. Recently, more elaborate methods to induce gene knockdown have been utilized. These include gene editing techniques such as CRISPR (46-48) which gives higher specificity and minimises off targets. Nevertheless, gene silencing using small interfering RNA (siRNA) should not be discounted altogether given its simplicity and reproducibility. Other factors that should be considered in gene silencing experiments for minimizing off targets include using more than one target siRNA for each targeted gene or having a mismatch control. Overexpression studies of MAPK1 merits further investigation and could be carried out to ascertain the link between RR and MAPK1. Furthermore, the expression of other partners in the Ras/Raf/MEK/ERK pathways could be explored both at the gene and protein levels to shed some mechanistic insight regarding the interactions between MAPK1, RR and leukemogenesis.

In conclusion, in the present study, we showed that MAPK1 simultaneously promotes myeloid cell proliferation and differentiation by cell cycle progression and blocking apoptosis. GO enrichment analysis showed that the processes involved in cell cycle, cell proliferation, and cell differentiation were affected by MAP1 downregulation.

Acknowledgements

Not applicable.

Funding

This study was supported by Research University grants 1001/CIPPT/812095 and 1001/CIPPT/813064 from Universiti Sains Malaysia.

Availability of data and materials

The datasets used during the present study are available from the corresponding author upon reasonable request.

Authors' contributions

SAASB, OH and NMY conceived and designed the study. SAASB performed the experiments. MS and EJM wrote the paper and analysed the data. EJM, NMY and OH reviewed and edited the manuscript. NMY funded the project. All authors read and approved the manuscript and agree to be accountable for all aspects of the research in ensuring that the accuracy or integrity of any part of the work are appropriately investigated and resolved.

Ethics approval and consent to participate

Not applicable.

Patient consent for publication

Not applicable.

Competing interests

The authors state that they have no competing interests.

References

1. Grimwade D, Hills RK, Moorman AV, Walker H, Chatters S, Goldstone AH, Wheatley K, Harrison CJ and Burnett AK; National Cancer Research Institute Adult Leukaemia Working Group: Refinement of cytogenetic classification in acute myeloid leukemia: Determination of prognostic significance of rare recurring chromosomal abnormalities among 5876 younger adult patients treated in the United Kingdom Medical Research Council trials. Blood 116: 354-365, 2010.
2. Nucifora G and Rowley JD: AML1 and the 8;21 and 3;21 translocations in acute and chronic myeloid leukemia. Blood 86: 1-14, 1995.

3. Miyoshi H, Kozu T, Shimizu K, Enomoto K, Maseki N, Kaneko Y, Kamada N and Ohki M: The t(8;21) translocation in acute myeloid leukemia results in production of an AML1-MTG8 fusion transcript. EMBO J 12: 2715-2721, 1993.
4. Chang KS, Fan YH, Stass SA, Estey EH, Wang G, Trujillo JM, Erickson P and Drabkin H: Expression of AML1-ETO fusion transcripts and detection of minimal residual disease in t(8;21)-positive acute myeloid leukemia. Oncogene 8: 983-988, 1993.
5. Heidenreich O, Krauter J, Riehle H, Hadwiger P, John M, Heil G, Vornlocher HP and Nordheim A: AML1/MTG8 oncogene suppression by small interfering RNAs supports myeloid differentiation of t(8;21)-positive leukemic cells. Blood 101: 3157-3163, 2003.
6. Trombly DJ, Whitfield TW, Padmanabhan S, Gordon JA, Lian JB, van Wijnen AJ, Zaidi SK, Stein JL and Stein GS: Genome-wide co-occupancy of AML1-ETO and N-CoR defines the t(8;21) AML signature in leukemic cells. BMC Genomics 16: 309, 2015.
7. Hildebrand D, Tiefenbach J, Heinzel T, Grez M and Maurer AB: Multiple regions of ETO cooperate in transcriptional repression. J Biol Chem 276: 9889-9895, 2001.
8. Yuan Y, Zhou L, Miyamoto T, Iwasaki H, Harakawa N, Hetherington CJ, Burel SA, Lagasse E, Weissman IL, Akashi K and Zhang DE: AML1-ETO expression is directly involved in the development of acute myeloid leukemia in the presence of additional mutations. Proc Natl Acad Sci USA 98: 10398-10403, 2001.
9. Maiques-Diaz A, Chou FS, Wunderlich M, Gómez-López G, Jacinto FV, Rodriguez-Perales S, Larrayoz MJ, Calasanz MJ, Mulloy JC, Cigudosa JC and Alvarez S: Chromatin modifications induced by the AML1-ETO fusion protein reversibly silence its genomic targets through AML1 and Sp1 binding motifs. Leukemia 26: 1329-1337, 2012.
10. Klampfer L, Zhang J, Zelenetz AO, Uchida H and Nimer SD: The AML1/ETO fusion protein activates transcription of BCL-2. Proc Natl Acad Sci USA 93: 14059-14064, 1996.
11. Linggi B, Müller-Tidow C, van de Locht L, Hu M, Nip J, Serve H, Berdel WE, van der Reijden B, Quelle DE, Rowley JD, *et al*: The t(8;21) fusion protein, AML1 ETO, specifically represses the transcription of the p14(ARF) tumor suppressor in acute myeloid leukemia. Nat Med 8: 743-750, 2002.
12. Vangala RK, Heiss-Neumann MS, Rangatia JS, Singh SM, Schoch C, Tenen DG, Hiddemann W and Behre G: The myeloid master regulator transcription factor PU.1 is inactivated by AML1-ETO in t(8;21) myeloid leukemia. Blood 101: 270-277, 2003.
13. Pabst T, Mueller BU, Harakawa N, Schoch C, Haferlach T, Behre G, Hiddemann W, Zhang DE and Tenen DG: AML1-ETO downregulates the granulocytic differentiation factor C/EBPalpha in t(8;21) myeloid leukemia. Nat Med 7: 444-451, 2001.
14. Rio-Machín A, Menezes J, Maiques-Diaz A, Agirre X, Ferreira BI, Acquadro F, Rodriguez-Perales S, Juaristi KA, Alvarez S and Cigudosa JC: Abrogation of RUNX1 gene expression in de novo myelodysplastic syndrome with t(4;21)(q21;q22). Haematologica 97: 534-537, 2012.
15. McCubrey JA, Steelman LS, Chappell WH, Abrams SL, Wong EW, Chang F, Lehmann B, Terrian DM, Milella M, Tafuri A, *et al*: Roles of the Raf/MEK/ERK pathway in cell growth, malignant transformation and drug resistance. Biochim Biophys Acta 1773: 1263-1284, 2007.
16. Morgan MA, Dolp O and Reuter CW: Cell-cycle-dependent activation of mitogen-activated protein kinase kinase (MEK-1/2) in myeloid leukemia cell lines and induction of growth inhibition and apoptosis by inhibitors of RAS signaling. Blood 97: 1823-1834, 2001.
17. Towatari M, Iida H, Tanimoto M, Iwata H, Hamaguchi M and Saito H: Constitutive activation of mitogen-activated protein kinase pathway in acute leukemia cells. Leukemia 11: 479-484, 1997.
18. Milella M, Kornblau SM, Estrov Z, Carter BZ, Lapillonne H, Harris D, Konopleva M, Zhao S, Estey E and Andreeff M: Therapeutic targeting of the MEK/MAPK signal transduction module in acute myeloid leukemia. J Clin Invest 108: 851-859, 2001.
19. Dhillon AS, Hagan S, Rath O and Kolch W: MAP kinase signalling pathways in cancer. Oncogene 26: 3279-3290, 2007.
20. Zaidi SK, Dowdy CR, van Wijnen AJ, Lian JB, Raza A, Stein JL, Croce CM and Stein GS: Altered Runx1 subnuclear targeting enhances myeloid cell proliferation and blocks differentiation by activating a miR-24/MKP-7/MAPK network. Cancer Res 69: 8249-8255, 2009.
21. Spirin PV, Lebedev TD, Orlova NN, Gornostaeva AS, Prokofjeva MM, Nikitenko NA, Dmitriev SE, Buzdin AA, Borisov NM, Aliper AM, *et al*: Silencing *AML1-ETO* gene expression leads to simultaneous activation of both pro-apoptotic and proliferation signaling. Leukemia 28: 2222-2228, 2014.
22. Dennis G Jr, Sherman BT, Hosack DA, Yang J, Gao W, Lane HC and Lempicki RA: DAVID: Database for annotation, visualization, and integrated discovery. Genome Biol 4: P3, 2003.
23. Huang da W, Sherman BT and Lempicki RA: Systematic and integrative analysis of large gene lists using DAVID bioinformatics resources. Nat Protoc 4: 44-57, 2009.
24. Huang da W, Sherman BT and Lempicki RA: Bioinformatics enrichment tools: Paths toward the comprehensive functional analysis of large gene lists. Nucleic Acids Res 37: 1-13, 2009.
25. Shih LY, Huang CF, Wang PN, Wu JH, Lin TL, Dunn P and Kuo MC: Acquisition of FLT3 or N-*ras* mutations is frequently associated with progression of myelodysplastic syndrome to acute myeloid leukemia. Leukemia 18: 466-475, 2004.
26. Bacher U, Haferlach T, Kern W, Haferlach C and Schnittger S: A comparative study of molecular mutations in 381 patients with myelodysplastic syndrome and in 4130 patients with acute myeloid leukemia. Haematologica 92: 744-752, 2007.
27. Martinez N, Drescher B, Riehle H, Cullmann C, Vornlocher HP, Ganser A, Heil G, Nordheim A, Krauter J and Heidenreich O: The oncogenic fusion protein RUNX1-CBFA2T1 supports proliferation and inhibits senescence in t(8;21)-positive leukaemic cells. BMC Cancer 4: 44, 2004.
28. Kikushige Y, Yoshimoto G, Miyamoto T, Iino T, Mori Y, Iwasaki H, Niiro H, Takenaka K, Nagafuji K, Harada M, *et al*: Human Flt3 is expressed at the hematopoietic stem cell and the granulocyte/macrophage progenitor stages to maintain cell survival. J Immunol 180: 7358-7367, 2008.
29. Ikeda H, Kanakura Y, Tamaki T, Kuriu A, Kitayama H, Ishikawa J, Kanayama Y, Yonezawa T, Tarui S and Griffin JD: Expression and functional role of the proto-oncogene c-kit in acute myeloblastic leukemia cells. Blood 78: 2962-2968, 1991.
30. Woźniak J and Kopeć-Szlezak J: c-Kit receptor (CD117) expression on myeloblasts and white blood cell counts in acute myeloid leukemia. Cytometry Part B Clin Cytometry 58: 9-16, 2004.
31. Stone RM, Mandrekar SJ, Sanford BL, Laumann K, Geyer S, Bloomfield CD, Thiede C, Prior TW, Döhner K, Marcucci G, *et al*: Midostaurin plus chemotherapy for acute myeloid leukemia with a *FLT3* mutation. N Engl J Med 377: 454-464, 2017.
32. Dong Chen, Waters SB, Holt KH and Pessin JE: SOS phosphorylation and disassociation of the Grb2-SOS complex by the ERK and JNK signaling pathways. J Biol Chem 271: 6328-6332, 1996.
33. Pedram A, Razandi M and Levin ER: Extracellular signal-regulated protein kinase/Jun kinase cross-talk underlies vascular endothelial cell growth factor-induced endothelial cell proliferation. J Biol Chem 273: 26722-26728, 1998.
34. Andreeff M, Jiang S, Zhang X, Konopleva M, Estrov Z, Snell VE, Xie Z, Okcu MF, Sanchez-Williams G, Dong J, *et al*: Expression of Bcl-2-related genes in normal and AML progenitors: Changes induced by chemotherapy and retinoic acid. Leukemia 13: 1881-1892, 1999.
35. Wang X: The expanding role of mitochondria in apoptosis. Genes Dev 15: 2922-2933, 2001.
36. Salvesen GS and Duckett CS: IAP proteins: Blocking the road to death's door. Nat Rev Mol Cell Biol 3: 401-410, 2002.
37. Westwick JK, Cox AD, Der CJ, Cobb MH, Hibi M, Karin M and Brenner DA: Oncogenic Ras activates c-Jun via a separate pathway from the activation of extracellular signal-regulated kinases. Proc Natl Acad Sci USA 91: 6030-6034, 1994.
38. Zhang P, Iwasaki-Arai J, Iwasaki H, Fenyus ML, Dayaram T, Owens BM, Shigematsu H, Levantini E, Huettner CS, Lekstrom-Himes JA, *et al*: Enhancement of hematopoietic stem cell repopulating capacity and self-renewal in the absence of the transcription factor C/EBP alpha. Immunity 21: 853-863, 2004.
39. Yamanaka R, Barlow C, Lekstrom-Himes J, Castilla LH, Liu PP, Eckhaus M, Decker T, Wynshaw-Boris A and Xanthopoulos KG: Impaired granulopoiesis, myelodysplasia, and early lethality in CCAAT/enhancer binding protein epsilon-deficient mice. Proc Natl Acad Sci USA 94: 13187-13192, 1997.
40. Wang H, Iakova P, Wilde M, Welm A, Goode T, Roesler WJ and Timchenko NA: C/EBPα arrests cell proliferation through direct inhibition of Cdk2 and Cdk4. Mol Cell 8: 817-828, 2001.

41. Ishiguro A, Spirin KS, Shiohara M, Tobler A, Gombart AF, Israel MA, Norton JD and Koeffler HP: Id2 expression increases with differentiation of human myeloid cells. Blood 87: 5225-5231, 1996.
42. Fujimoto T, Anderson K, Jacobsen SE, Nishikawa Si and Nerlov C: Cdk6 blocks myeloid differentiation by interfering with Runx1 DNA binding and Runx1-C/EBPalpha interaction. EMBO J 26: 2361-2370, 2007.
43. Rangatia J, Vangala RK, Treiber N, Zhang P, Radomska H, Tenen DG, Hiddemann W and Behre G: Downregulation of c-Jun expression by transcription factor C/EBPα is critical for granulocytic lineage commitment. Mol Cell Biol 22: 8681-8694, 2002.
44. Shivakumar L, Minna J, Sakamaki T, Pestell R and White MA: The RASSF1A tumor suppressor blocks cell cycle progression and inhibits cyclin D1 accumulation. Mol Cell Biol 22: 4309-4318, 2002.
45. Kearsey JM, Coates PJ, Prescott AR, Warbrick E and Hall PA: Gadd45 is a nuclear cell cycle regulated protein which interacts with p21Cip1. Oncogene 11: 1675-1683, 1995.
46. Ding Q, Regan SN, Xia Y, Oostrom LA, Cowan CA and Musunuru K: Enhanced efficiency of human pluripotent stem cell genome editing through replacing TALENs with CRISPRs. Cell Stem Cell 12: 393-394, 2013
47. Shafie NH, Saleem M, Moses EJ, Razak SR and Yusoff NM: The CRISPR-Cas9 system: A new dawn in gene editing. J Bioanalys Biomed 6: 45-48, 2014.
48. Kleinstiver BP, Pattanayak V, Prew MS, Tsai SQ, Nguyen NT, Zheng Z and Joung JK: High-fidelity CRISPR-Cas9 nucleases with no detectable genome-wide off-target effects. Nature 529: 490-495, 2016.